Auxiliary material for paper …

Assessing the consistency between short-term global temperature trends in observations and climate model projections

Patrick J. Michaels
George Mason University
4400 University Drive, Fairfax, Virginia 22030
pmichaels@cato.org

Paul C. Knappenberger
New Hope Environmental Services, Inc.
536 Pantops Center, #402
Charlottesville, Virginia 22911
chip@nhes.com

John R. Christy
Earth System Science Center, NSSTC
University of Alabama in Huntsville
Huntsville, Virginia 35805
john.christy@nsstc.uah.edu

Chad S. Herman
Marlboro, New Jersey
chad.herman.us@gmail.com

Lucia. M. Liljegren
Lisle, Illinois
lucia@rankexploits.com

James D. Annan
Research Institute for Global Change
Yokohama, Japan
jdannan@jamstec.go.jp

Auxiliary Methods

1. Climate Model Selection

Gridded monthly projections of surface and atmospheric air temperatures from 51 individual climate model runs representing 20 separate climate models were downloaded from the PCMDI CMIP3 model archive database. Model selection consisted of only those listed in IPCC AR4 Table 10.4. and runs whose 20C3M runs continue forward with SRES A1B. Of these models, two had to be eliminated. There was no atmospheric temperature data available for MIUB ECHO-G so lower troposphere temperatures could not be simulated. CNRM CM 3 was eliminated because the netCDF files did not represent the atmospheric temperature on a consistent set of pressure levels.

The models and the numbers of runs we used in our analysis are included in Table 1 (details of these climate models can be found at the PCMDI archive, http://www-pcmdi.llnl.gov/ipcc/model_documentation/ipcc_model_documentation.php).

Table 1. Model names and number of available runs.

Model Name	Number of Runs
BCCR BCM 2.0	1
CCCMA CGCM 3.1 T47	5
CCCMA CGCM 3.1 T63	1
CSIRO MK 3.0	1
ECHAM5/MPI-OM	4
GFDL CM 2.0	1
GFDL CM 2.1	1
GISS AOM	2
GISS EH	3
GISS ER	5
IAP FGOALS 1.0g	3

INM CM 3.0	1
IPSL CM 4	1
MIROC 3.2 HIRES	1
MIROC 3.2 MEDRES	3
MRI CGCM 2.3.2a	5
NCAR CCSM 3.0	7
NCAR PCM 1	4
UKMO HAD CM 3	1
UKMO HADGEM 1	1

2. Creation of monthly surface air temperature anomalies

For each model run, the projected monthly gridded surface air temperature values were spatially averaged to produce global average temperatures for each month. The global average monthly temperatures were then converted to global average monthly temperature anomalies by subtracting the climatology for each model run over the period January 2001 through December 2020.

3. Creation of monthly synthetic MSU lower troposphere temperatures anomalies

Microwave Sounder Units (MSU) carried aboard a series of NASA satellites monitor bulk average temperatures in the atmosphere. A temperature for the lower troposphere can be generated from the MSU observations by a weighted combination of several MSU frequency channels. To properly compare the observed MSU lower troposphere temperatures with climate model projections, model-generated atmosphere temperature data must be used to develop an equivalent synthetic MSU lower troposphere temperature product. To this end, we employed the procedure described by Santer et al. [1999] as implemented by Santer and Doutriaux [2005] as part of the PCMDI Climate Data Analysis Tools package to produce gridded monthly, synthetic MSU lower troposphere temperatures from each model run. The gridded temperature values were spatially averaged to produce global average temperatures for each month. The global average monthly temperatures were then converted to global average monthly temperature anomalies by subtracting the climatology for each model run over the period January 2001 through December 2020.

References

Santer, B., and C. Doutriaux, 2005. Subroutine MSUWEIGHTS3.f, Part of the Climate Data Analysis Tools available from the Lawrence Livermore National Laboratory’s (LLNL) Program for Climate Model Diagnosis and Intercomparison (PCMDI), http://www2pcmdi.llnl.gov/svn/repository/cdat/tags/CDAT4.3/contrib/MSU/Src/msuweight.f and archived at http://www.webcitation.org/5owusvk91.

Santer, B. D., J. J. Hnilo, T. M. L. Wigley, J. S. Boyle, C. Doutriaux, M. Fiorino, D. E. Parker, and K. E. Taylor (1999), Uncertainties in observationally based estimates of temperature change in the free atmosphere, J. Geophys. Res., 104(D6), 6305–6333.

4. Accounting for “observational error”

Observations of the average global temperature contain uncertainties that model projected temperatures do not. These “observational errors” include such things as incomplete spatial coverage, changing number of stations within gridcells, changing observational practices, etc. The magnitude of these errors has been quantified in the literature describing each of the observed datasets that we used in our study. For the UAH MSU lower troposphere temperatures, the standard errors for the monthly anomalies are given in Christy et al [2003]. Brohan et al. [2008] describes the monthly components of observational error that are contained in the HadCRUT3 surface temperatures. For the GISS [Hansen et al., 2006] and NCDC [Smith et al., 2008] surface temperatures, however, only the standard error of the annual anomalies are presented. The information quantifying the errors of monthly global anomalies in the RSS MSU lower troposphere temperatures was obtained through personal communications [Mears, 2010].

Since we are using monthly anomalies, we require estimates of the errors for monthly anomalies. The Hadley Center website (http://hadobs.metoffice.com/hadcrut3/diagnostics/global/nh+sh/) provides global temperature anomalies as well as error ranges for the HadCRUT3 dataset, for both monthly and annual anomalies. If the errors were independent from one another at the monthly timescale, the annual error would be equal to the monthly error divided by the square root of 12 (or by a factor of 3.46). However, comparing the listed monthly and annual error ranges, we find that the annual error in the HadCRUT3 is only reduced by a factor of 1.73 from the monthly errors (or the square root of 3), indicating that the errors are not independent (Table 2). The major source of observational error in the global temperature anomalies complied in the HadCRUT3 data is a result of incomplete spatial coverage, with a minor contribution from bias [Brohan et al., 2008]. The error resulting from bias has a lower-frequency variability than does the error from incomplete spatial coverage [Brohan et al., 2008].

Since we have only estimates of the error of the annual global anomalies available from the GISS [Hansen et al., 2006] and the NCDC [Smith et al., 2008] datasets, we will use the HadCRUT monthly-to-annual scaling factor to guide our estimation of the error about the monthly anomalies reported in the NCDC and GISS datasets. Smith et al. [2008] finds that in the NCDC dataset, the contribution from bias is greater than the contribution from incomplete spatial coverage, as they use interpolation to increase the spatial coverage of the observations. Since bias error is more temporally correlated than error resulting from incomplete spatial coverage, we reduce the scaling factor that we determined from the HadCRUT3 data from 1.73 down to 1.50 for the NCDC dataset to account for the likely reduced degrees of freedom in the NCDC error compared with HadCRUT3 errors. As the characteristics of the spatial coverage of the GISS data are similar to that of the NCDC data, we apply the 1.50 scaling factor to the GISS data as well. The reported annual error, along with our estimated monthly error for these datasets is listed in Table 2.

Table 2. The standard error of "observational errors" of the annual and monthly global temperature anomalies from the 5 observed datasets used in our analysis.

Dataset	Annual Error (°C)	Monthly Error (°C)
HadCRUT3*	0.045	0.078
NCDC	0.03	0.045
GISS	0.025	0.0375
UAH MSU	0.075	0.10
RSS MSU	0.043	0.047

*This is an average for the HadCRUT3 errors (over 1979-2009) as the actual errors are computed monthly and differ from month to month

To assess the influence of these observational errors on the trends of length 5 to 15 years ending in December 2009 in each dataset, we used a Monte Carlo simulation, drawing each monthly data element randomly from a normal distribution with a mean equal to the observed monthly global temperature anomaly, and a standard deviation equal to the monthly error listed in Table 1 (for the HadCRUT3 data, we used the error explicitly as reported on the Hadley Center web site, http://hadobs.metoffice.com/hadcrut3/diagnostics/global/nh+sh/, which differs from month to month). We performed 10,000 replications for each series (from 5 to 15 years in length ending in December 2009) for each dataset, determining the linear least-squares trend through each. From the distributions of 10,000 values for each trend length for each dataset, we determined the standard deviation representing the trend variability due to observational errors assuming independence from month to month. The effect of correlations in the monthly errors was not assessed. The likelihood that the correlations in monthly errors vary considerably in time and across datasets makes it difficult to speculate whether the trend variability would be higher or lower than we determined assuming error independence on the specific 5 to 15 years trends in this study.

We incorporated the influence of observational into our distributions of model trends by adding the standard deviation from observational error determined for each trend length and each observational dataset as described above, in quadrature to the standard deviation of the model trend distributions of the same length, $\sigma_{x+y} = \mathrm{sqrt}(\sigma_x^2+\sigma_y^2)$, where σ_{x+y} is the combined standard deviation, σ_x^2 is the standard deviation of the model trend distributions, and σ_y^2 is the standard deviation of observational error. Each distribution of modeled trends was broadened by the inclusion of the effect of observational errors.

Auxiliary Table 1. Value of the linear least-squares trend for lengths ranging from 5 years (60 months) to 15 years (180 months) through global average temperature anomalies ending in December 2009, from the five observed datasets used in this study.

			Trend (°C/yr)		
Trend Length (yrs)	GISS	HADCRUT3	NCDC	UAH MSU v5.2	RSS MSU v3.2
5	-0.01835	-0.01608	-0.01564	-0.03560	-0.04033
6	-0.00178	-0.01409	-0.00773	-0.01573	-0.02256
7	-0.00205	-0.01445	-0.00782	-0.01451	-0.02412
8	-0.00365	-0.01325	-0.00735	-0.01615	-0.02147
9	0.00169	-0.00761	-0.00242	-0.00797	-0.01232
10	0.01214	0.00292	0.00689	0.00542	0.00154
11	0.01783	0.00733	0.01037	0.01203	0.00882
12	0.01099	-0.00001	0.00511	-0.00283	-0.00522
13	0.01224	0.00226	0.00590	0.00395	0.00149
14	0.01556	0.00957	0.01189	0.00873	0.00715
15	0.01526	0.01061	0.01217	0.00937	0.00785

Auxiliary Figure 1.

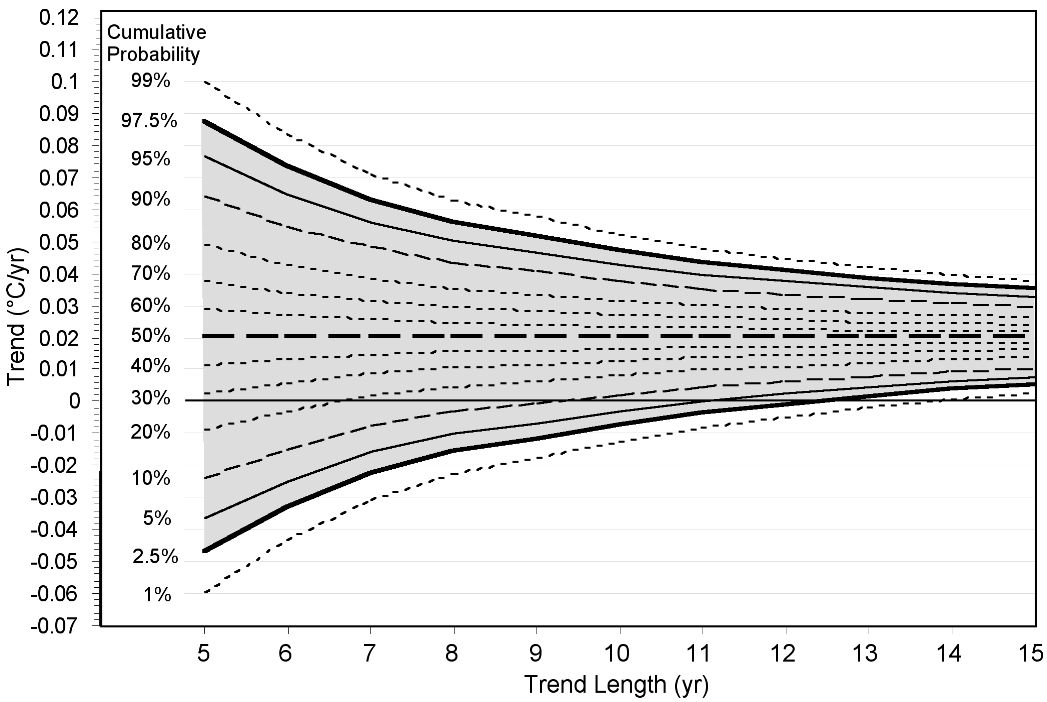

Auxiliary Figure 1. Cumulative probability distribution of trend values for trends ranging in length from 5 to 15 years derived from 20 models under SRES A1B for the period January 2001 through December 2020 for global average MSU lower troposphere temperatures. The 95% confidence range is shaded in grey and a zero trend is indicated by the horizontal black line.